ARR No. L5F08a

NATIONAL ADVISORY COMMITTEE FOR AERONAUTICS

WARTIME REPORT

ORIGINALLY ISSUED
July 1945 as
Advance Restricted Report L5F08a

COLUMN AND PLATE COMPRESSIVE STRENGTHS OF AIRCRAFT STRUCTURAL MATERIALS

EXTRUDED 75S-T ALUMINUM ALLOY

By George J. Heimerl and J. Albert Roy

Langley Memorial Aeronautical Laboratory
Langley Field, Va.

WASHINGTON

NATIONAL ADVISORY COMMITTEE FOR AERONAUTICS

ADVANCE RESTRICTED REPORT

COLUMN AND PLATE COMPRESSIVE STRENGTHS OF AIRCRAFT STRUCTURAL MATERIALS

EXTRUDED 75S-T ALUMINUM ALLOY

By George J. Heimerl and J. Albert Roy

SUMMARY

Column and plate compressive strengths of extruded 75S-T aluminum alloy were determined both within and beyond the elastic range from tests of thin-strip columns and local-instability tests of H-, Z-, and channel-section columns. These tests are part of an extensive research investigation to provide data on the structural strength of various aircraft materials. The results, which are presented in the form of curves and charts that are suitable for use in the design and analysis of aircraft structures, supersede preliminary results published previously.

INTRODUCTION

Column and plate members in an aircraft structure are the basic elements that fail by instability. For the design of lightweight, structurally efficient aircraft, the strength of these elements must be known for the various aircraft materials. An extensive research program has therefore been undertaken at the Langley Memorial Aeronautical Laboratory to establish the column and plate compressive strengths of a number of the alloys available for use in aircraft structures. Parts of this investigation already completed are given for 24S-T and 17S-T aluminum-alloy sheet in references 1 and 2, respectively.

The results of tests to determine the column and plate compressive strengths of extruded 75S-T aluminum alloy, which supersede preliminary results published in reference 3, are presented herein.

SYMBOLS

L length of column

ρ radius of gyration

c fixity coefficient used in Euler column formula

$\frac{L}{\rho\sqrt{c}}$ effective slenderness ratio of thin-strip column

b_F, t_F width and thickness, respectively, of flange of H-, Z-, or channel section (see fig. 1)

b_W, t_W width and thickness, respectively, of web of H-, Z-, or channel section (see fig. 1)

r corner radius (see fig. 1)

k_W nondimensional coefficient used with b_W and t_W in plate-buckling formula (see figs. 2 and 3 and reference 4)

E_c modulus of elasticity in compression, taken as 10,500 ksi for extruded 75S-T aluminum alloy

τ nondimensional coefficient (The value of τ is so determined that, when the effective modulus τE_c is substituted for E_c in the equation for elastic buckling of columns, the computed critical stress agrees with the experimentally observed value. The coefficient τ is equal to unity within the elastic range and decreases with increasing stress beyond the elastic range.)

η nondimensional coefficient for compressed plates corresponding to τ for columns

μ Poisson's ratio, taken as 0.3 for extruded 75S-T aluminum alloy

σ_{cr} critical compressive stress

$\bar{\sigma}_{max}$ average compressive stress at maximum load

σ_{cy} compressive yield stress

METHODS OF TESTING AND ANALYSIS

All tests were made in hydraulic testing machines accurate within three-fourths of 1 percent. The methods of testing and analysis developed for this research program are described in reference 1 and may be briefly summarized as follows:

The compressive stress-strain curves, which identify the material for correlation with its column and plate compressive strengths, were obtained for the with-grain direction from tests of single-thickness compression specimens cut from the extruded H-sections. These tests were made in a compression fixture of the Montgomery-Templin type, which provides lateral support through closely spaced rollers.

The column strength and the associated effective column modulus were obtained for the with-grain direction by the use of the method presented in reference 5, in which thin-strip columns of the material were tested with the ends clamped in fixtures that provide a high degree of end restraint. The fixtures used have been improved and the method of analysis has been modified since publication of reference 5. The method now used results in a column curve that is representative of nearly perfect column specimens. In addition, the method now takes into account the fact that columns of the dimensions tested are actually plates with two free edges. These columns were cut from the flanges of the extruded H-section adjacent to the junction of the web and flange.

The plate compressive strength of the material was obtained from compression tests of H-, Z-, and channel-section columns so proportioned as to develop local instability, that is, instability of the plate elements. (See fig. 4.) The extruded H-sections were obtained in three different web widths; the flange widths of each were varied by milling off parts of the flanges. The flanges of some of the H-section extrusions were removed in such a way as to make both Z- and channel sections. The flange widths of the Z- and channel-section columns were varied in the same manner as the flange widths for the H-section columns. The lengths of the columns were selected in accordance with the principles set forth in reference 6. The columns were tested with the ends ground flat and square and bearing directly against the testing-machine heads. In these local-instability tests measurements were taken of the cross-sectional distortion, and the critical stress was determined as the stress at the point near the top of the knee of the stress-distortion curve at which a marked increase in distortion first occurred with small increase in stress.

A difference in the analysis presented herein from that employed in reference 1 is concerned with the measurement of b_F and b_W for use in evaluating σ_{cr}/η by means of the equations and curves of figures 2 and 3. In the theoretical derivation of the plate-buckling formula mathematically idealized sections were assumed, in which the effects of the thickness of the flange and web plate elements and the effect of the corner condition - square, curved, or fillet - were neglected in establishing the widths of the plate elements. Consequently, as the experimental investigation of the plate compressive strength of aircraft materials progresses, some arbitrary dimensioning of the flange and web widths has been found necessary in order that the theoretical and experimental buckling stresses agree within the elastic range. In the formed Z- and channel sections of references 1 and 2 with inside bend radius of three times the sheet thickness, the widths of the flange and web were defined by center-line widths with square corners assumed. In the extruded sections with small fillets reported herein, the widths of the flange and web were defined by the inside face dimensions, as shown in figure 1.

RESULTS AND DISCUSSION

Compressive Stress-Strain Curves

Compressive stress-strain curves for extruded 75S-T aluminum alloy, which were selected as typical or average curves for the column material, are given in figure 5. These curves were obtained from tests of compression specimens cut from the middle part of the flanges of the extrusions as shown in figure 5.

In order to study the variation of the compressive properties over the cross section of an H-section extrusion, surveys were made by tests of compression specimens cut from the web and flanges of the H-sections. The variation of the compressive yield stress σ_{cy} over the cross section is shown in figure 6. Values of σ_{cy} at the outer part of the flanges were generally higher than those for the inner part of the flanges; the lowest value of σ_{cy} was found in the web in all cases. The stress-strain curves of figure 5, representative of the material in the middle part of the flanges, are therefore usually typical or average curves for the flange material and show values of σ_{cy} that are unconservative in comparison with values of the compressive yield stress for the material in the web.

The thin-strip or H-, Z-, and channel-section columns to which a particular stress-strain curve applies are indicated in table 1 together with the values of σ_{cy} for that stress-strain curve. The values of σ_{cy} have an average of about 79 ksi for the with-grain direction. The modulus of elasticity in compression was taken as 10,500 ksi, the present accepted value for extruded 75S-T aluminum alloy.

Column and Plate Compressive Strengths

Because the compressive properties of an extruded aluminum alloy may vary considerably, the data and charts of this report should not be used for design purposes for extrusions of 75S-T aluminum alloy that have appreciably different compressive properties from those reported herein, unless a suitable method is devised for adjusting test results to account for variations in material properties. The results of the column and local-instability tests of the extruded 75S-T aluminum alloy are summarized herein; a discussion of the basic relationships is given in reference 1.

Column strength.- The column curve of figure 7 shows the results of tests of thin-strip columns loaded in the with-grain direction. The reduction of the effective modulus of elasticity τE_c with the increase in column stress is indicated by the variation of τ with stress shown in figure 8.

Plate compressive strength.- The results of the local-instability tests of the H-, Z-, and channel-section columns used to determine the plate compressive strength are given in tables 2, 3, and 4, respectively. The plate-buckling curves, analogous to the column curve of figure 7, are shown in figure 9. The reduction of the effective modulus of elasticity ηE_c with the increase in stress for plates is indicated by the variation of η with stress, which is shown together with the curve for τ, in figure 8. In this figure, the τ-curve does not cross the η-curves as it did for 24S-T aluminum alloy. (See fig. 12 of reference 1.) The extruded H-, Z-, and channel-section columns of 75S-T aluminum alloy apparently were more nearly perfect than the formed Z- and channel-section columns of 24S-T aluminum alloy (reference 1), so that the η-curves for the extruded 75S-T aluminum-alloy columns diverge from unity at about the same point as the τ-curve, which is representative of nearly perfect columns.

The variation of the actual critical stress σ_{cr} with the theoretical critical stress σ_{cr}/η computed for elastic buckling by means of the formulas and curves of figures 2 and 3 is shown in figure 10. In order to illustrate the difference between the critical stress σ_{cr} and the average stress at maximum load $\bar{\sigma}_{max}$, the variation of σ_{cr} with $\sigma_{cr}/\bar{\sigma}_{max}$ is shown in figure 11. Because values of $\bar{\sigma}_{max}$ may be required in strength calculations, the variation of $\bar{\sigma}_{max}$ with σ_{cr}/η is presented in figure 12.

Figures 9 to 12 show that the data for H-sections described curves different from those indicated for Z- and channel sections. One of the reasons why higher values of $\bar{\sigma}_{max}$ were obtained for the H-sections than for the Z- and channel sections for a given value of σ_{cr}/η (fig. 12) may be the fact that the high-strength material in the flanges forms a higher percentage of the total cross-sectional area for the H-section than for the Z- or channel section. For the H-section, $\bar{\sigma}_{max}$ is increased over the value for the Z- or channel section for the entire stress range covered in these tests (fig. 12); σ_{cr} for the H-section, however, is increased only for stresses beyond the elastic range (fig. 10).

For the variation of σ_{cr} with $\sigma_{cr}/\bar{\sigma}_{max}$ (fig. 11) and of $\bar{\sigma}_{max}$ with σ_{cr}/η (fig. 12), only a single curve is required for a given type of cross section regardless of the value of b_W/t_W; whereas, in the corresponding figures 15 and 16 of reference 1, separate curves were necessary for different values of this ratio. This distinction is probably due to the fact that there is no increase in the compressive yield stress in the corners of the extruded sections comparable with the increase in the corners of formed specimens caused by the cold work of forming the shapes from flat sheet. Reference 1 shows how the increased strength in the curved corners due to forming might produce a variation in the average stress at maximum load when b_W/t_W is varied.

Langley Memorial Aeronautical Laboratory
National Advisory Committee for Aeronautics
Langley Field, Va.

REFERENCES

1. Lundquist, Eugene E., Schuette, Evan H., Heimerl, George J., and Roy, J. Albert: Column and Plate Compressive Strengths of Aircraft Structural Materials. 24S-T Aluminum-Alloy Sheet. NACA ARR No. L5F01, 1945.

2. Heimerl, George J., and Roy, J. Albert: Column and Plate Compressive Strengths of Aircraft Structural Materials. 17S-T Aluminum-Alloy Sheet. NACA ARR No. L5F08, 1945.

3. Heimerl, George J., and Roy, J. Albert: Column and Plate Compressive Strength of Extruded XB75S-T Aluminum Alloy. NACA RB No. L4E26, 1944.

4. Kroll, W. D., Fisher, Gordon P., and Heimerl, George J.: Charts for Calculation of the Critical Stress for Local Instability of Columns with I-, Z-, Channel, and Rectangular-Tube Section. NACA ARR No. 3K04, 1943.

5. Lundquist, Eugene E., Rossman, Carl A., and Houbolt, John C.: A Method for Determining the Column Curve from Tests of Columns with Equal Restraints against Rotation on the Ends. NACA TN No. 903, 1943.

6. Heimerl, George J., and Roy, J. Albert: Determination of Desirable Lengths of Z- and Channel-Section Columns for Local-Instability Tests. NACA RB No. L4H10, 1944.

TABLE 1

COMPRESSIVE PROPERTIES OF EXTRUDED 75S-T ALUMINUM ALLOY

[E_c = 10,500 ksi]

Columns to which stress-strain curves apply		Stress-strain curve (fig. 5)	Compressive yield stress, σ_{cy} (ksi)
Type	Designation (tables 2 to 4)		
Thin strip	All	A	77.5
H	1a to 3b, 5a to 5c, 7a to 8b, 10 to 11c	B	78.6
H	13a to 17c	C	81.6
H	18a to 23a	D	79.3
H	23b, 23c	E	79.1
H	4a to 4c, 6a to 6c, 9a to 9c, 12a to 12c	F	78.1
Z	1a to 3b	G	79.1
Z	4a, 4b, 5b	H	78.4
Z	5a, 6a to 6c	I	78.7
Z	7a to 8b	E	79.1
Z	9a to 9c	A	77.5
Channel	1a to 3c	G	79.1
Channel	4a to 5c	H	78.4
Channel	6a to 6c	I	78.7
Channel	7a to 8c	E	79.1
Channel	9a, 9b	A	77.5

TABLE 2.- DIMENSIONS AND TEST RESULTS FOR H-SECTION COLUMNS

THAT DEVELOP LOCAL INSTABILITY

Column	t_W (in.)	t_F (in.)	b_W (in.)	b_F (in.)	L (in.)	$\frac{L}{b_W}$	$\frac{t_W}{t_F}$	$\frac{b_W}{t_W}$	$\frac{b_F}{b_W}$	k_W (fig. 2)	$\frac{b_W}{t_W}\sqrt{\frac{12(1-\mu^2)}{k_W}}$	$\frac{\sigma_{cr}}{\eta}$ (ksi) (a)	σ_{cr} (ksi)	$\bar{\sigma}_{max}$ (ksi)	$\frac{\sigma_{cr}}{\bar{\sigma}_{max}}$
1a	0.120	0.126	1.61	0.82	6.10	3.79	0.95	13.42	0.512	2.72	26.9	143.3	79.3	82.5	0.961
1b	.121	.126	1.61	.80	6.10	3.79	.96	13.34	.500	2.78	26.5	148.3	77.2	82.6	.935
1c	.120	.125	1.62	.82	6.10	3.76	.96	13.46	.505	2.73	26.9	143.0	78.2	83.1	.941
2a	.120	.126	1.61	.90	6.05	3.75	.96	13.44	.559	2.38	28.8	123.0	78.7	80.1	.983
2b	.120	.126	1.62	.90	6.07	3.75	.96	13.46	.558	2.38	28.8	122.2	78.3	80.3	.975
3a	.121	.126	1.62	.98	6.10	3.76	.96	13.43	.608	2.02	31.3	106.3	76.8	77.4	.992
3b	.121	.126	1.62	.99	6.08	3.75	.96	13.43	.610	2.02	31.3	106.3	77.0	77.7	.995
4a	.120	.121	1.62	.99	8.75	5.40	.99	13.45	.613	1.92	32.0	100.7	75.1	76.4	.983
4b	.121	.121	1.62	.99	8.75	5.40	1.00	13.36	.612	1.91	32.0	101.6	76.3	77.5	.985
4c	.121	.121	1.62	.99	8.75	5.40	.99	13.42	.611	1.91	32.1	100.7	74.4	76.9	.967
5a	.121	.126	1.62	1.03	6.49	4.01	.96	13.41	.636	1.87	32.4	98.7	76.0	76.3	.996
5b	.120	.126	1.62	1.03	6.52	4.02	.96	13.49	.633	1.89	32.4	98.5	75.5	76.4	.988
5c	.120	.126	1.62	1.03	6.46	3.99	.96	13.44	.636	1.88	32.4	98.7	76.5	77.3	.990
6a	.121	.121	1.62	1.08	8.75	5.40	1.00	13.37	.671	1.62	34.8	86.0	74.1	74.7	.992
6b	.121	.122	1.62	1.09	8.76	5.41	1.00	13.40	.669	1.63	34.8	86.2	73.8	75.5	.977
6c	.121	.121	1.62	1.08	8.76	5.41	1.00	13.36	.669	1.63	34.6	86.6	73.8	74.7	.988
7a	.121	.126	1.62	1.16	6.93	4.28	.96	13.41	.716	1.52	35.9	80.2	71.8	72.6	.989
7b	.121	.126	1.62	1.17	7.00	4.32	.96	13.43	.720	1.52	36.0	80.0	71.7	72.2	.993
7c	.121	.126	1.62	1.18	7.01	4.33	.96	13.41	.727	1.49	36.3	78.6	72.0	72.5	.993
8a	.120	.126	1.61	1.16	7.82	4.86	.96	13.36	.724	1.48	36.3	78.7	70.8	72.5	.977
8b	.121	.126	1.62	1.17	7.80	4.81	.95	13.42	.723	1.50	36.2	79.0	71.1	72.5	.981
9a	.121	.121	1.62	1.17	10.10	6.23	.99	13.40	.723	1.42	37.2	75.1	70.9	71.5	.992
9b	.121	.121	1.62	1.17	10.10	6.23	1.00	13.39	.723	1.42	37.1	75.2	69.0	70.4	.980
9c	.120	.121	1.62	1.17	10.10	6.23	.99	13.45	.724	1.42	37.3	74.5	68.5	70.9	.966
10	.121	.126	1.62	1.25	7.82	4.83	.96	13.42	.772	1.33	38.5	70.1	69.0	69.6	.991
11a	.121	.127	1.61	1.34	8.72	5.42	.95	13.28	.834	1.17	40.7	63.0	62.0	65.6	.945
11b	.121	.127	1.61	1.34	8.71	5.41	.95	13.27	.834	1.17	40.6	63.1	61.6	65.2	.945
11c	.121	.127	1.61	1.34	8.71	5.41	.95	13.31	.831	1.18	40.5	63.2	62.4	64.1	.973
12a	.121	.122	1.62	1.34	10.75	6.64	.99	13.41	.829	1.14	42.1	60.1	61.9	63.7	.972
12b	.120	.121	1.62	1.34	10.80	6.67	.99	13.45	.830	1.14	42.2	59.9	61.8	63.2	.978
12c	.120	.122	1.62	1.34	10.80	6.67	.99	13.45	.829	1.14	42.2	59.9	61.2	63.2	.968
13a	.120	.123	2.23	1.26	11.62	5.21	.97	18.69	.562	2.29	40.8	62.2	59.5	61.5	.967
13b	.119	.123	2.23	1.26	11.61	5.21	.97	18.73	.562	2.29	40.9	61.9	59.7	61.8	.966
13c	.119	.123	2.23	1.26	11.60	5.20	.97	18.74	.564	2.26	41.2	61.0	59.9	61.6	.972
14a	.119	.123	2.24	1.36	12.59	5.62	.97	18.78	.608	2.00	43.9	53.8	53.2	57.8	.920
14b	.119	.123	2.23	1.37	12.63	5.66	.97	18.73	.611	2.00	43.8	54.1	53.1	57.6	.922
14c	.119	.123	2.23	1.36	12.63	5.66	.97	18.71	.611	2.00	43.7	54.2	53.1	57.7	.920
15a	.119	.123	2.24	1.43	13.30	5.94	.97	18.78	.638	1.84	45.8	49.5	50.3	56.0	.898
15b	.119	.123	2.23	1.43	13.30	5.96	.97	18.71	.638	1.84	45.6	49.9	51.0	56.1	.909
15c	.119	.123	2.23	1.43	13.31	5.97	.97	18.74	.638	1.84	45.7	49.8	50.3	56.3	.893
16a	.119	.123	2.23	1.60	13.82	6.20	.97	18.76	.718	1.51	50.5	40.7	41.9	53.7	.780
16b	.119	.123	2.23	1.59	13.83	6.20	.97	18.73	.714	1.52	50.2	41.1	42.1	53.8	.783
16c	.119	.123	2.23	1.59	13.81	6.19	.97	18.73	.714	1.52	50.2	41.1	41.9	53.7	.780
17a	.119	.125	2.23	1.84	14.70	6.59	.95	18.71	.824	1.19	56.8	32.3	31.3	51.2	.611
17b	.120	.125	2.23	1.84	14.73	6.61	.96	18.66	.824	1.19	56.7	32.4	32.2	51.5	.625
17c	.119	.125	2.24	1.84	14.66	6.54	.95	18.75	.822	1.19	56.9	32.1	32.9	51.8	.635
18a	.123	.121	2.74	1.16	11.49	4.19	1.02	22.22	.425	3.19	41.1	61.3	61.8	62.9	.983
18b	.123	.121	2.76	1.14	11.49	4.16	1.01	22.48	.412	3.37	40.5	62.3	61.2	63.6	.962
19a	.122	.121	2.74	1.24	12.98	4.74	1.01	22.36	.454	2.95	43.1	56.0	54.9	57.8	.950
19b	.123	.121	2.73	1.24	13.00	4.76	1.02	22.30	.453	2.95	43.0	56.3	56.2	58.6	.959
19c	.122	.120	2.73	1.22	13.01	4.77	1.01	22.35	.448	3.00	42.7	57.0	58.5	59.4	.985
20a	.122	.119	2.74	1.37	14.40	5.26	1.02	22.47	.502	2.50	47.0	47.0	45.4	54.3	.836
20b	.122	.120	2.74	1.37	14.41	5.26	1.02	22.50	.501	2.50	47.0	46.9	48.3	55.0	.878
20c	.122	.120	2.74	1.38	14.40	5.26	1.02	22.46	.504	2.50	46.9	47.0	47.6	54.8	.869
21a	.122	.119	2.74	1.67	15.21	5.55	1.02	22.48	.608	1.83	54.9	34.3	35.5	51.8	.685
21b	.122	.120	2.74	1.67	15.18	5.54	1.02	22.46	.608	1.83	54.8	34.4	33.7	51.1	.659
21c	.122	.120	2.74	1.68	15.19	5.54	1.02	22.50	.612	1.84	54.0	34.4	35.2	51.3	.686
22a	.122	.120	2.74	1.96	16.72	6.11	1.02	22.42	.718	1.37	63.2	25.9	26.4	49.1	.538
22b	.122	.119	2.74	1.96	16.70	6.09	1.02	22.45	.717	1.37	63.3	25.8	26.0	49.0	.530
23a	.122	.120	2.74	2.24	17.80	6.50	1.02	22.48	.817	1.10	70.8	20.6	20.2	47.0	.430
23b	.123	.122	2.74	2.24	17.79	6.49	1.02	22.23	.820	1.09	70.3	20.9	21.5	47.9	.449
23c	.124	.122	2.74	2.24	17.81	6.50	1.01	22.16	.818	1.10	69.8	21.3	21.9	47.9	.457

[a] $\frac{\sigma_{cr}}{\eta} = \frac{k_W \pi^2 E_c t_W^2}{12(1-\mu^2) b_W^2}$, where E_c = 10,500 ksi and μ = 0.3.

NATIONAL ADVISORY
COMMITTEE FOR AERONAUTICS

TABLE 3.- DIMENSIONS AND TEST RESULTS FOR Z-SECTION COLUMNS

THAT DEVELOP LOCAL INSTABILITY

Column	t_W (in.)	t_F (in.)	b_W (in.)	b_F (in.)	L (in.)	$\frac{L}{b_W}$	$\frac{t_W}{t_F}$	$\frac{b_W}{t_W}$	$\frac{b_F}{b_W}$	k_W (fig.3)	$\frac{b_W}{t_W}\sqrt{\frac{12(1-\mu^2)}{k_W}}$	$\frac{\sigma_{cr}}{\eta}$ (ksi) (a)	σ_{cr} (ksi)	$\bar{\sigma}_{max}$ (ksi)	$\frac{\sigma_{cr}}{\bar{\sigma}_{max}}$
1a	0.120	0.125	1.63	1.07	6.13	3.76	0.96	13.61	0.658	2.00	31.8	102.4	72.1	73.7	0.979
1b	.120	.125	1.62	1.06	6.10	3.76	.96	13.48	.657	2.00	31.5	104.4	73.8	74.6	.989
1c	.120	.127	1.62	1.07	6.11	3.77	.95	13.45	.662	2.01	31.3	105.4	73.7	74.7	.987
2a	.120	.127	1.62	1.17	7.01	4.32	.95	13.49	.721	1.74	33.7	90.8	71.2	72.5	.982
2b	.120	.125	1.62	1.16	6.99	4.31	.96	13.50	.715	1.74	33.8	90.6	71.3	72.0	.990
2c	.120	.127	1.62	1.17	6.97	4.30	.95	13.46	.724	1.72	33.9	90.1	70.0	72.2	.969
3a	.121	.127	1.62	1.34	8.73	5.39	.95	13.41	.829	1.36	38.1	71.7	66.0	67.2	.982
3b	.120	.125	1.62	1.34	8.75	5.40	.96	13.47	.828	1.34	38.5	70.1	63.8	66.4	.961
4a	.120	.124	2.25	1.31	11.90	5.29	.97	18.74	.581	2.42	39.9	65.4	59.8	61.7	.969
4b	.120	.125	2.25	1.31	11.90	5.29	.97	18.73	.582	2.41	39.7	65.2	60.1	62.3	.965
5a	.117	.122	2.26	1.58	13.80	6.11	.96	19.23	.702	1.81	47.3	46.4	45.2	53.2	.850
5b	.120	.123	2.25	1.58	13.77	6.12	.98	18.76	.702	1.76	46.9	47.5	45.1	53.6	.842
6a	.118	.124	2.27	1.85	14.70	6.48	.95	19.23	.814	1.39	53.8	35.6	34.3	50.1	.685
6b	.119	.123	2.26	1.85	14.70	6.50	.96	19.11	.817	1.37	53.9	35.6	35.6	50.3	.708
7a	.122	.121	2.76	1.36	14.41	5.22	1.01	22.68	.492	2.93	43.8	54.1	53.1	55.8	.952
7b	.122	.121	2.76	1.37	14.40	5.22	1.01	22.59	.496	2.85	44.3	53.0	52.7	56.0	.941
8a	.122	.120	2.76	1.78	16.11	5.84	1.02	22.58	.644	1.87	54.6	34.8	35.4	49.9	.709
8b	.123	.121	2.76	1.78	16.11	5.84	1.02	22.47	.644	1.87	54.4	35.1	36.0	49.4	.729
9a	.122	.120	2.78	2.25	17.90	6.44	1.02	22.77	.810	1.25	67.4	22.9	23.4	45.9	.510
9b	.122	.120	2.78	2.25	17.90	6.44	1.02	22.71	.810	1.25	67.2	23.1	22.8	45.8	.498
9c	.121	.120	2.78	2.26	17.90	6.44	1.01	23.01	.813	1.29	67.0	23.2	23.3	45.8	.509

[a] $\frac{\sigma_{cr}}{\eta} = \frac{k_W \pi^2 E_c t_W^2}{12(1-\mu^2) b_W^2}$, where E_c = 10,500 ksi and μ = 0.3.

NATIONAL ADVISORY

COMMITTEE FOR AERONAUTICS

TABLE 4.- DIMENSIONS AND TEST RESULTS FOR CHANNEL-SECTION COLUMNS

THAT DEVELOP LOCAL INSTABILITY

Column	t_W (in.)	t_F (in.)	b_W (in.)	b_F (in.)	L (in.)	$\frac{L}{b_W}$	$\frac{t_W}{t_F}$	$\frac{b_W}{t_W}$	$\frac{b_F}{b_W}$	k_W (fig. 3)	$\frac{b_W}{t_W}\sqrt{\frac{12(1-\mu^2)}{k_W}}$	$\frac{\sigma_{cr}}{\eta}$ (ksi) (a)	σ_{cr} (ksi)	$\bar{\sigma}_{max}$ (ksi)	$\frac{\sigma_{cr}}{\bar{\sigma}_{max}}$
1a	0.121	0.126	1.62	1.08	6.12	3.78	0.96	13.41	0.666	1.96	31.7	103.4	73.8	74.6	0.989
1b	.121	.127	1.62	1.08	6.15	3.79	.95	13.41	.667	1.96	31.7	103.4	73.4	74.6	.984
2a	.120	.126	1.62	1.17	7.00	4.32	.95	13.48	.720	1.71	34.1	89.3	68.1	72.2	.943
2b	.121	.126	1.61	1.16	7.01	4.36	.96	13.34	.722	1.71	33.8	91.2	69.4	73.1	.949
2c	.120	.126	1.62	1.17	7.00	4.32	.95	13.44	.720	1.71	34.0	89.8	69.8	72.6	.961
3a	.121	.126	1.61	1.33	8.75	5.43	.96	13.30	.827	1.34	38.0	71.9	66.0	68.0	.971
3b	.120	.126	1.62	1.34	8.75	5.40	.96	13.45	.825	1.36	38.2	71.3	65.2	67.1	.972
3c	.120	.126	1.62	1.33	8.74	5.40	.96	13.49	.821	1.37	38.0	71.4	65.9	67.6	.975
4a	.120	.124	2.21	1.36	11.91	5.39	.97	18.39	.613	2.22	40.8	62.3	59.4	60.5	.982
4b	.121	.124	2.23	1.36	11.92	5.35	.97	18.52	.607	2.25	41.0	62.2	58.5	59.6	.982
4c	.121	.124	2.23	1.35	11.92	5.35	.97	18.51	.607	2.25	41.0	62.3	57.5	59.7	.963
5a	.120	.124	2.23	1.58	13.82	6.20	.97	18.56	.708	1.72	46.8	47.4	46.8	54.3	.862
5b	.120	.123	2.23	1.59	13.82	6.20	.98	18.58	.711	1.72	46.8	47.3	46.5	52.9	.879
5c	.120	.124	2.23	1.59	13.81	6.19	.97	18.59	.710	1.72	46.8	47.2	46.0	52.5	.876
6a	.118	.122	2.24	1.83	14.70	6.56	.97	18.91	.820	1.36	53.8	36.1	35.6	49.1	.725
6b	.119	.123	2.24	1.84	14.70	6.56	.97	18.84	.824	1.35	53.7	36.1	35.4	49.1	.721
6c	.118	.123	2.24	1.83	14.70	6.56	.97	18.88	.820	1.36	53.6	36.2	35.6	49.3	.722
7a	.122	.120	2.73	1.36	14.40	5.27	1.02	22.28	.500	2.83	43.9	54.1	54.2	55.5	.977
7b	.122	.120	2.72	1.36	14.39	5.29	1.02	22.30	.499	2.83	43.9	54.0	54.0	56.4	.957
8a	.122	.121	2.74	1.82	16.10	5.88	1.01	22.40	.663	1.81	55.1	34.2	34.7	49.5	.701
8b	.122	.120	2.74	1.81	16.10	5.88	1.01	22.45	.661	1.81	55.2	34.1	34.5	47.3	.729
8c	.123	.120	2.74	1.81	16.10	5.88	1.02	22.35	.661	1.79	55.2	34.1	35.3	47.8	.739
9a	.123	.120	2.74	2.22	17.95	6.55	1.02	22.31	.808	1.26	65.8	24.0	24.3	44.5	.546
9b	.123	.120	2.74	2.23	17.95	6.55	1.02	22.35	.812	1.25	66.2	23.7	24.3	46.2	.526

[a] $\frac{\sigma_{cr}}{\eta} = \frac{k_W \pi^2 E_c t_W^2}{12(1-\mu^2) b_W^2}$, where E_c = 10,500 ksi and μ = 0.3.

NATIONAL ADVISORY

COMMITTEE FOR AERONAUTICS

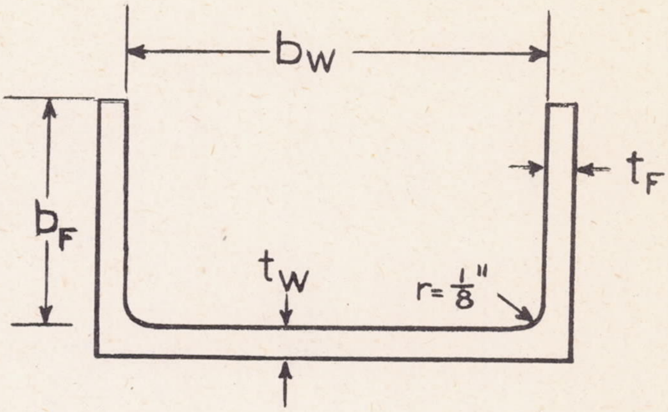

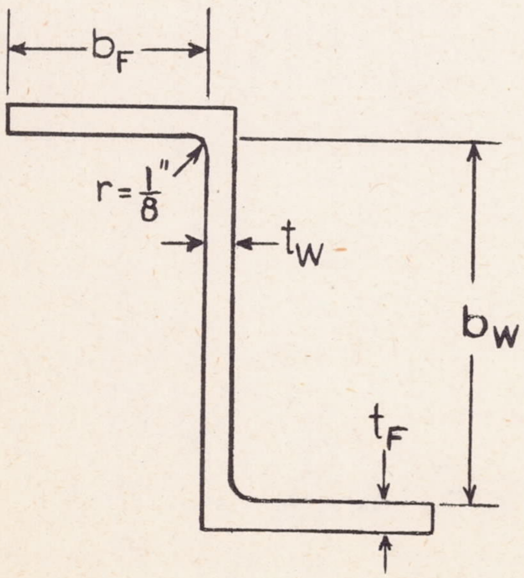

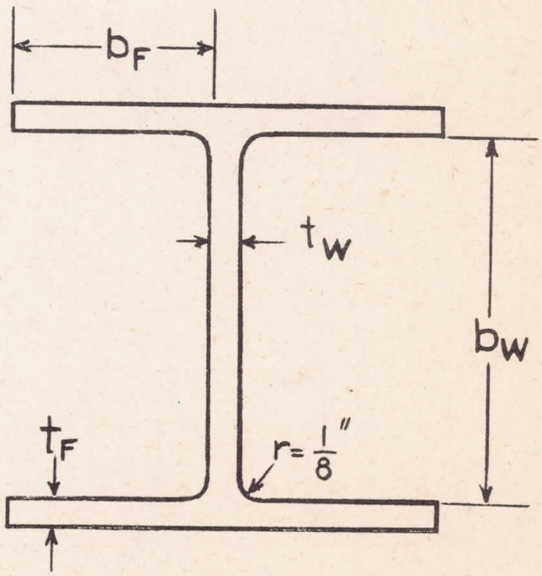

NATIONAL ADVISORY
COMMITTEE FOR AERONAUTICS

Figure 1.- Cross sections of H-, Z-, and channel-section columns.

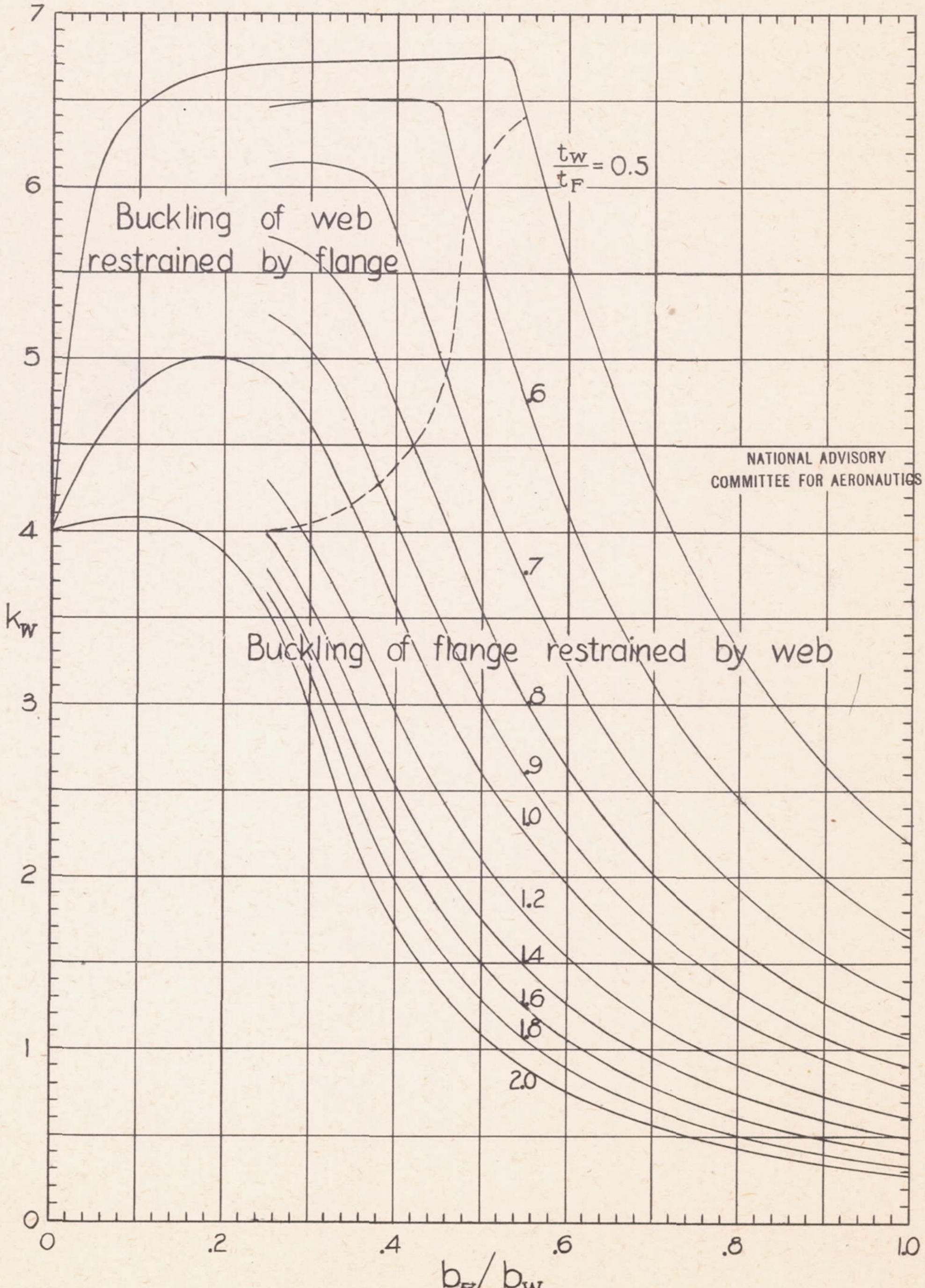

Figure 2.- Values of k_W for H-section columns. (From reference 4.)

$$\frac{\sigma_{cr}}{\eta} = \frac{k_W \pi^2 E_c t_W^2}{12(1-\mu^2) b_W^2}$$

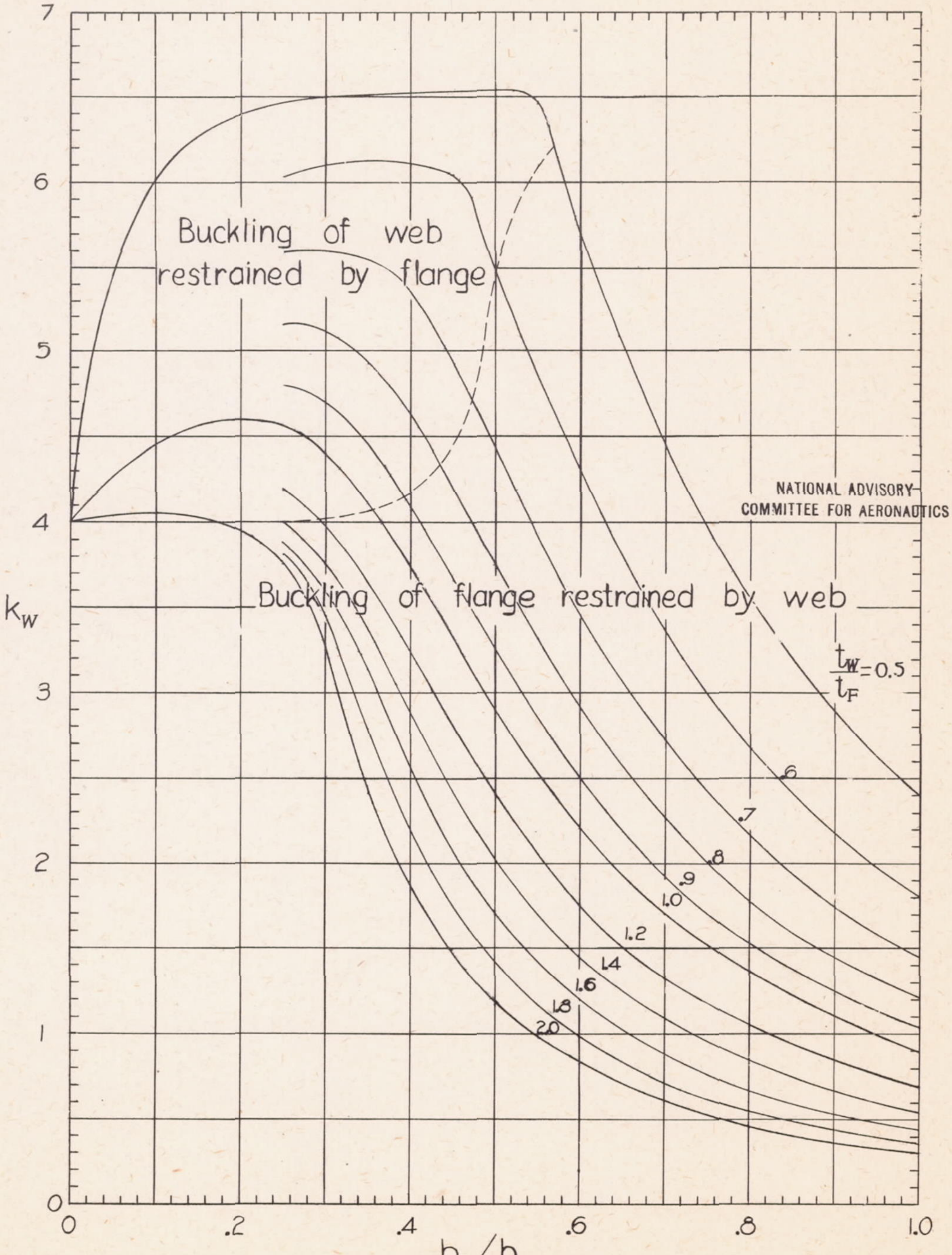

Figure 3.- Values of k_W for Z-and channel-section columns. (From reference 4.)

$$\frac{\sigma_{cr}}{\eta} = \frac{k_W \pi^2 E_c t_W^2}{12(1-\mu^2) b_W^2}$$

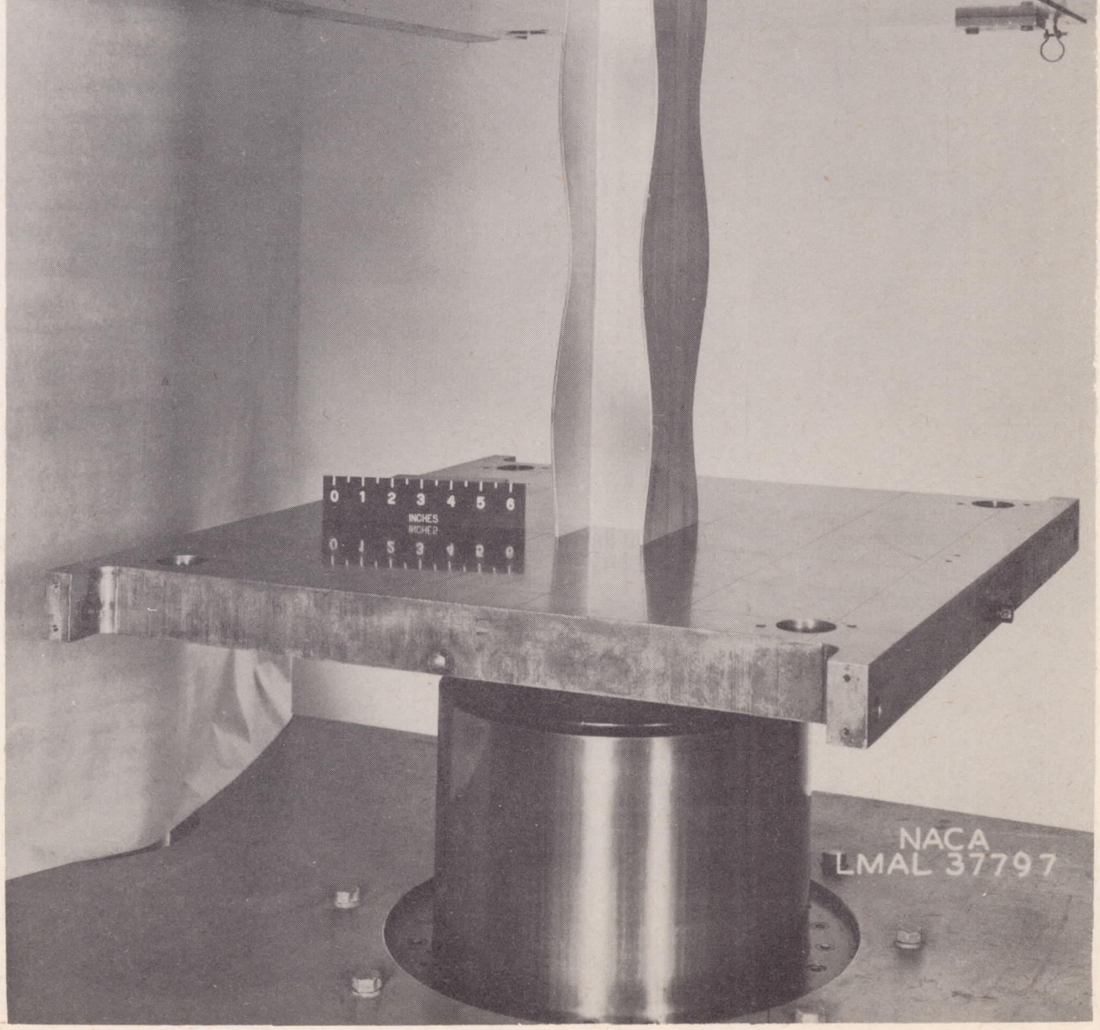

Figure 4.- Local instability of an H-section column.

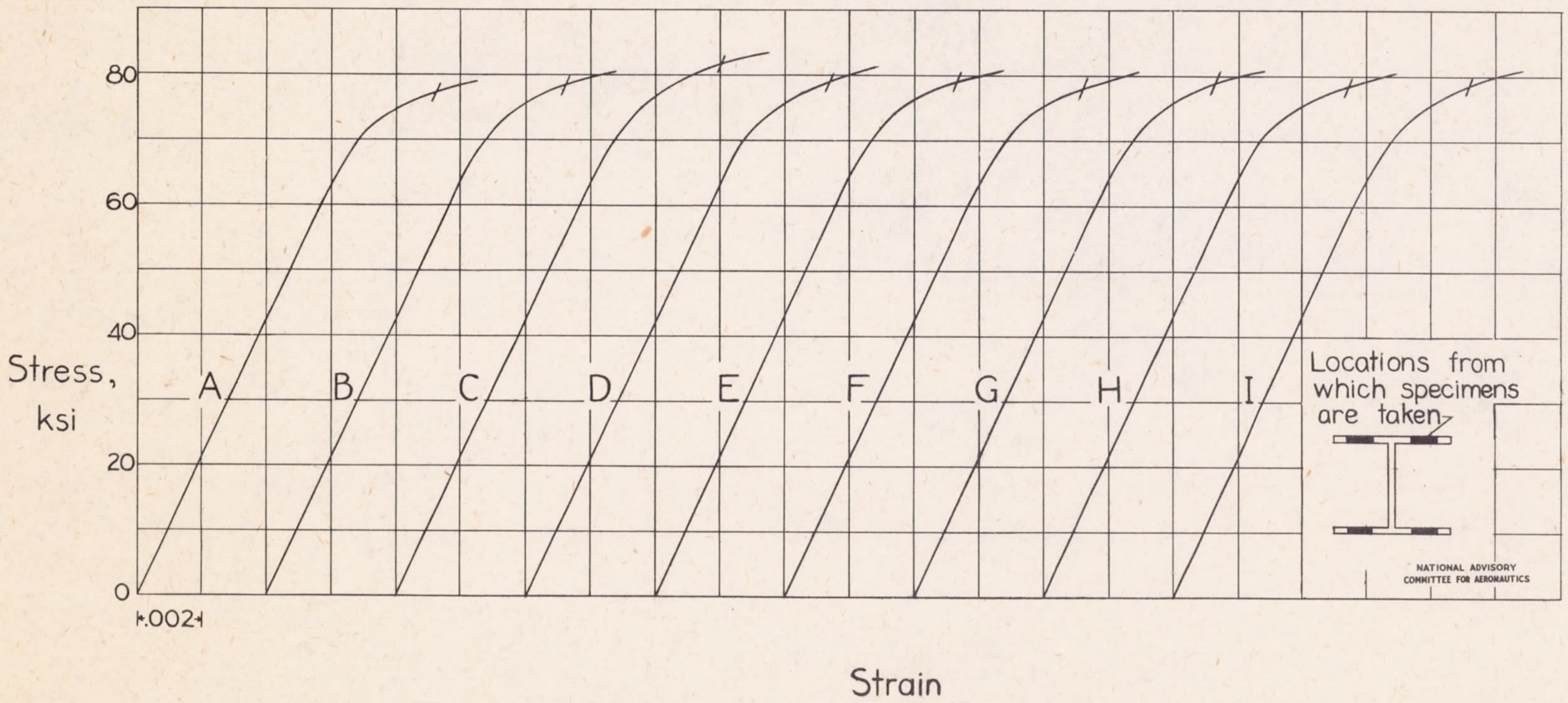

Figure 5. – Compressive stress-strain curves for extruded 75S-T aluminum alloy. (Curves A, B, C, etc. are identified in table 1.)

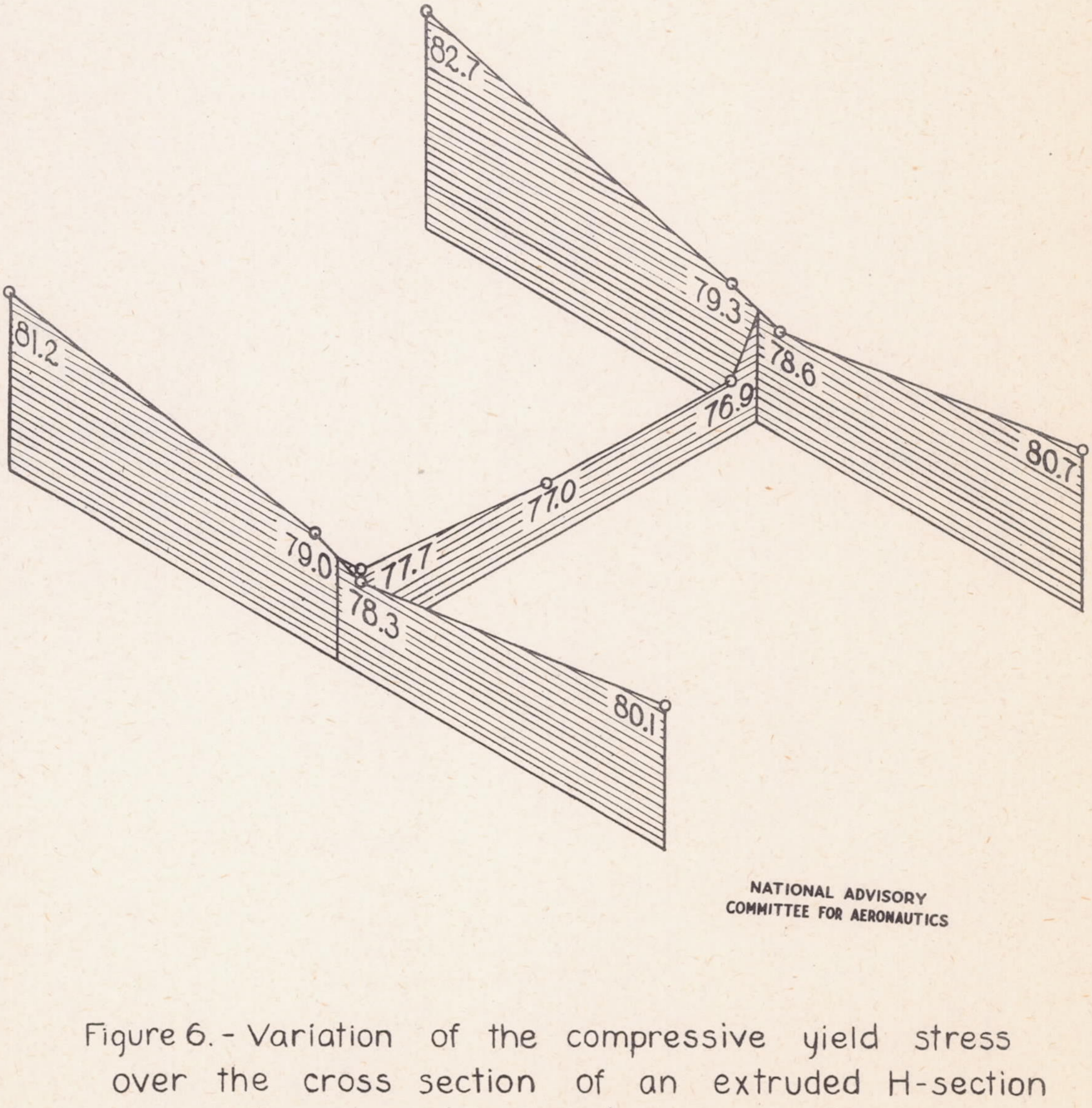

Figure 6.- Variation of the compressive yield stress over the cross section of an extruded H-section of 75S-T aluminum alloy. (Values in ksi.)

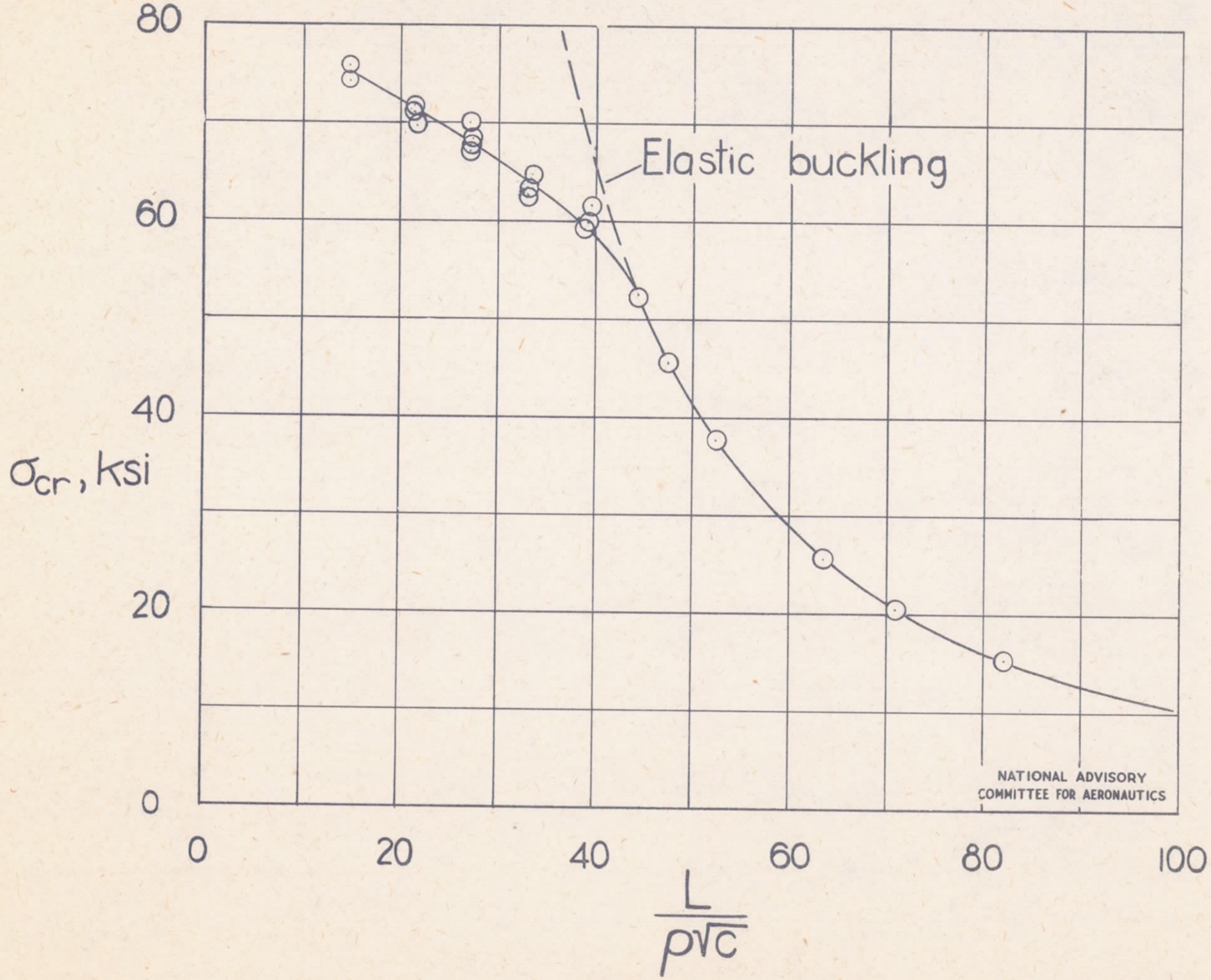

Figure 7. Column curve for extruded 75 S-T aluminum alloy obtained from tests of thin-strip columns. $\sigma_{cy} = 77$ ksi.

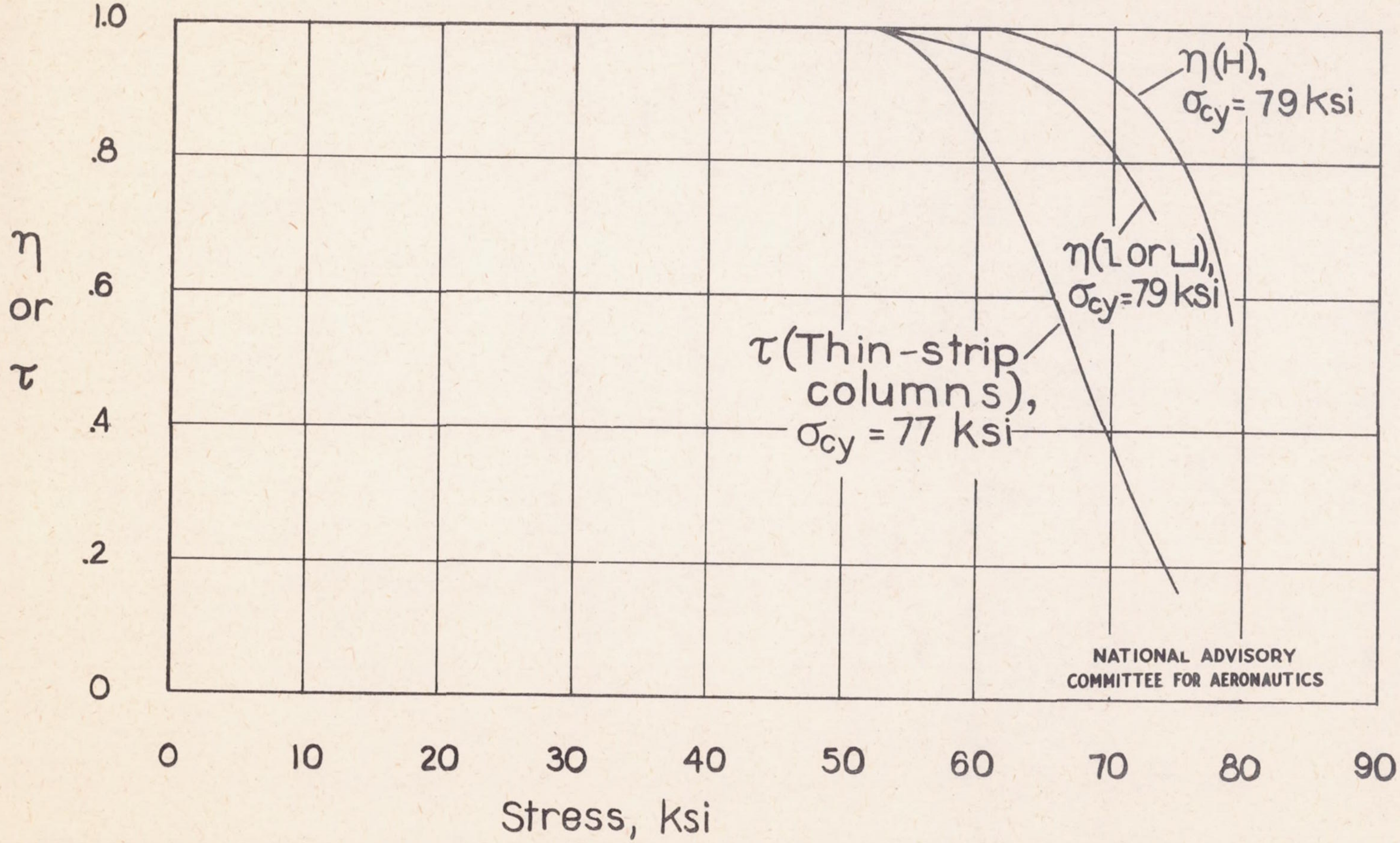

Figure 8. - Variation of η and τ with stress for extruded 75 S-T aluminum alloy.

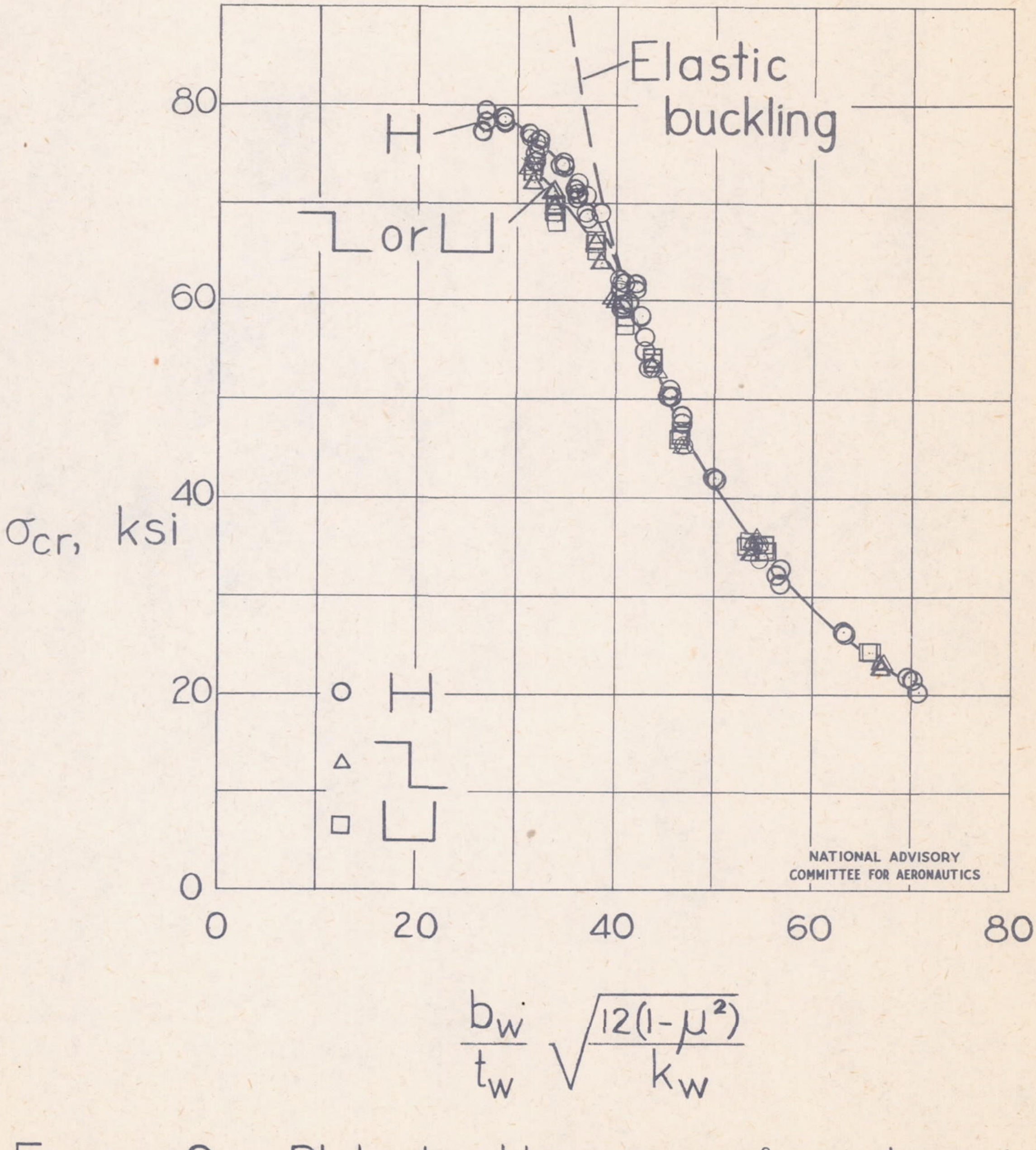

Figure 9.- Plate-buckling curve for extruded 75S-T aluminum alloy obtained from tests of H-, Z-, and channel-section columns. σ_{cy} = 79 ksi.

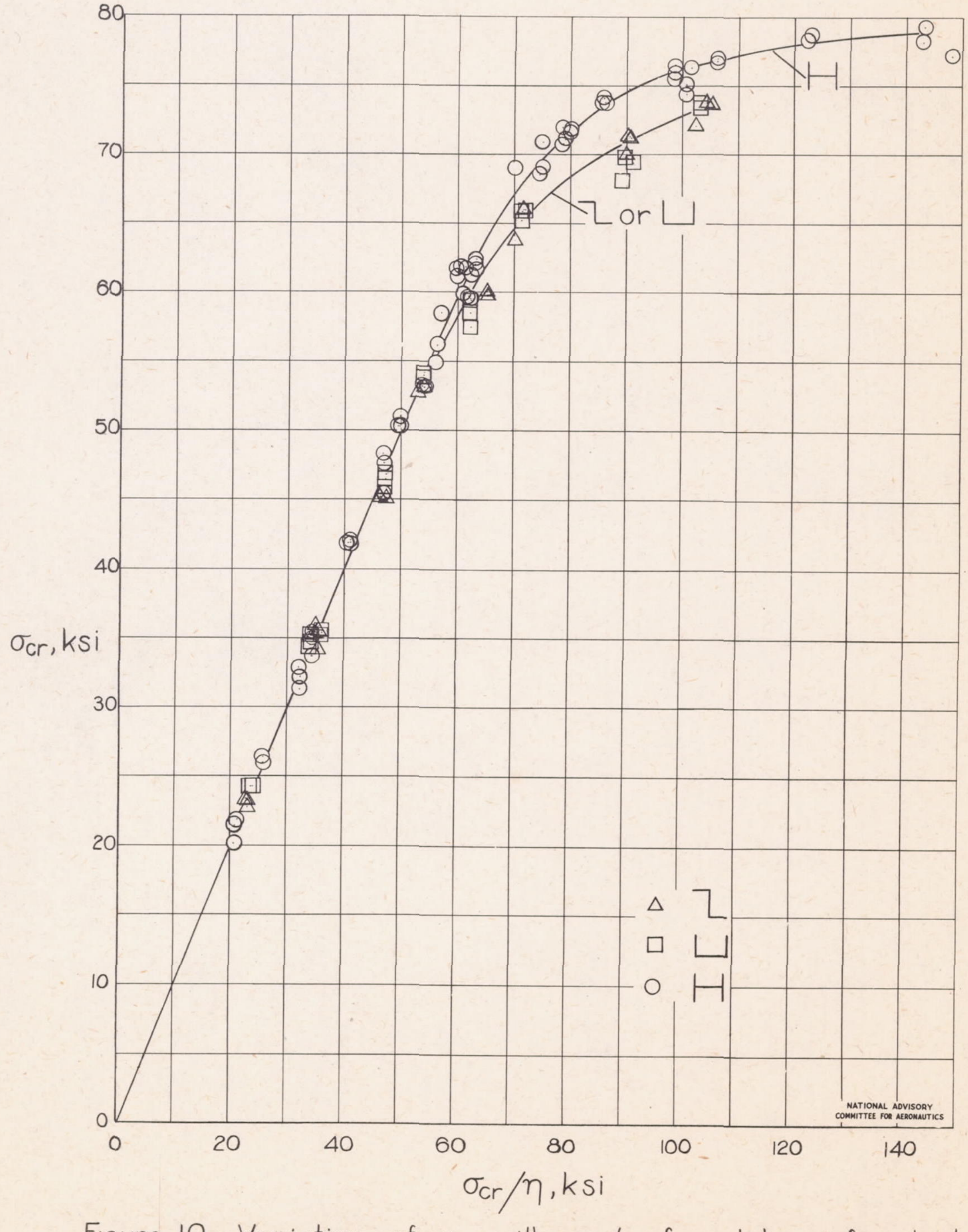

Figure 10.- Variation of σ_{cr} with σ_{cr}/η for plates of extruded 75S-T aluminum alloy obtained from tests of H-, Z-, and channel-section columns. σ_{cy} = 79 ksi.

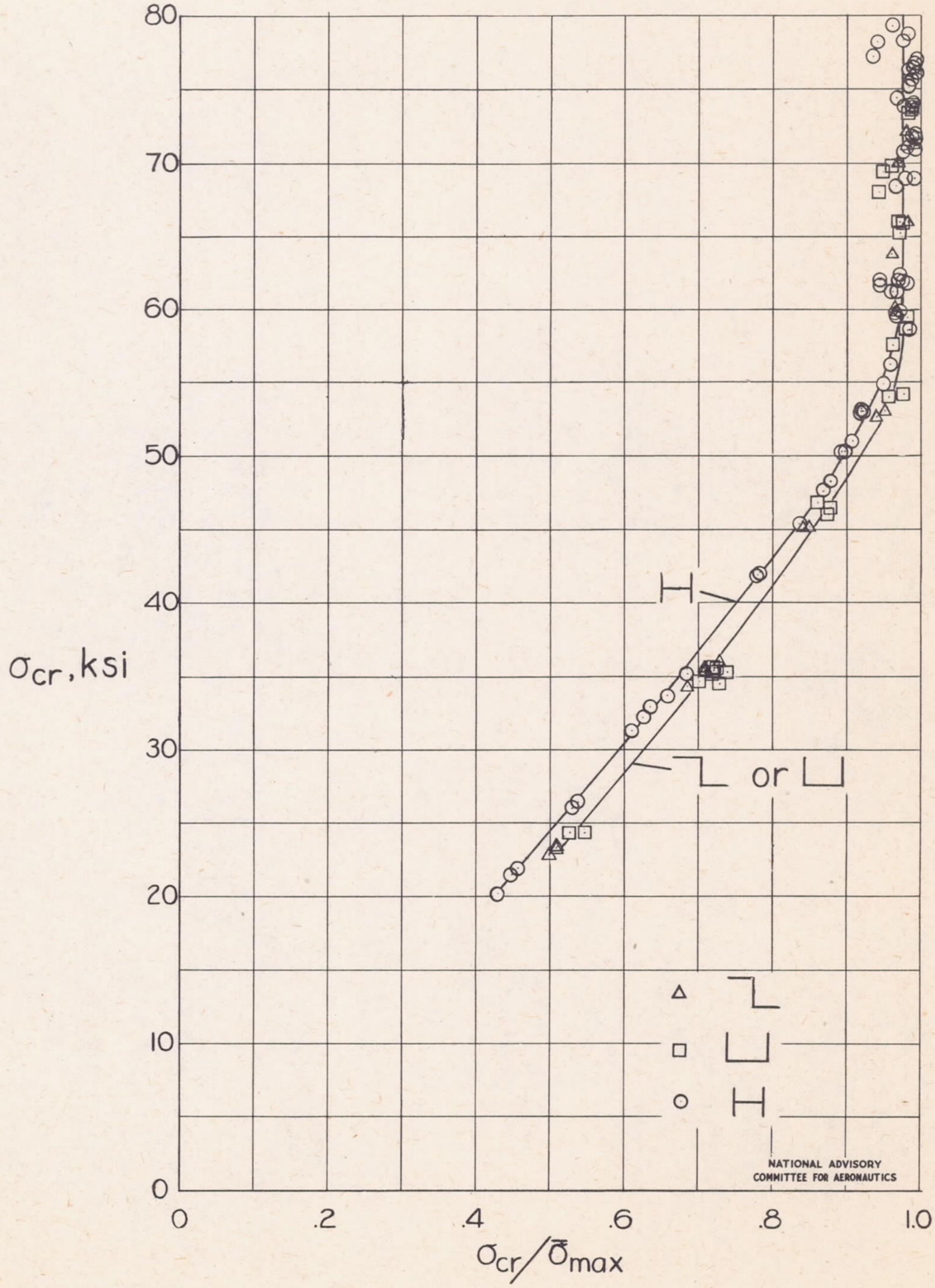

Figure 11.- Variation of σ_{cr} with $\sigma_{cr}/\bar{\sigma}_{max}$ for plates of extruded 75S-T aluminum alloy obtained from tests of H-, Z-, and channel-section columns. σ_{cy} = 79 ksi.

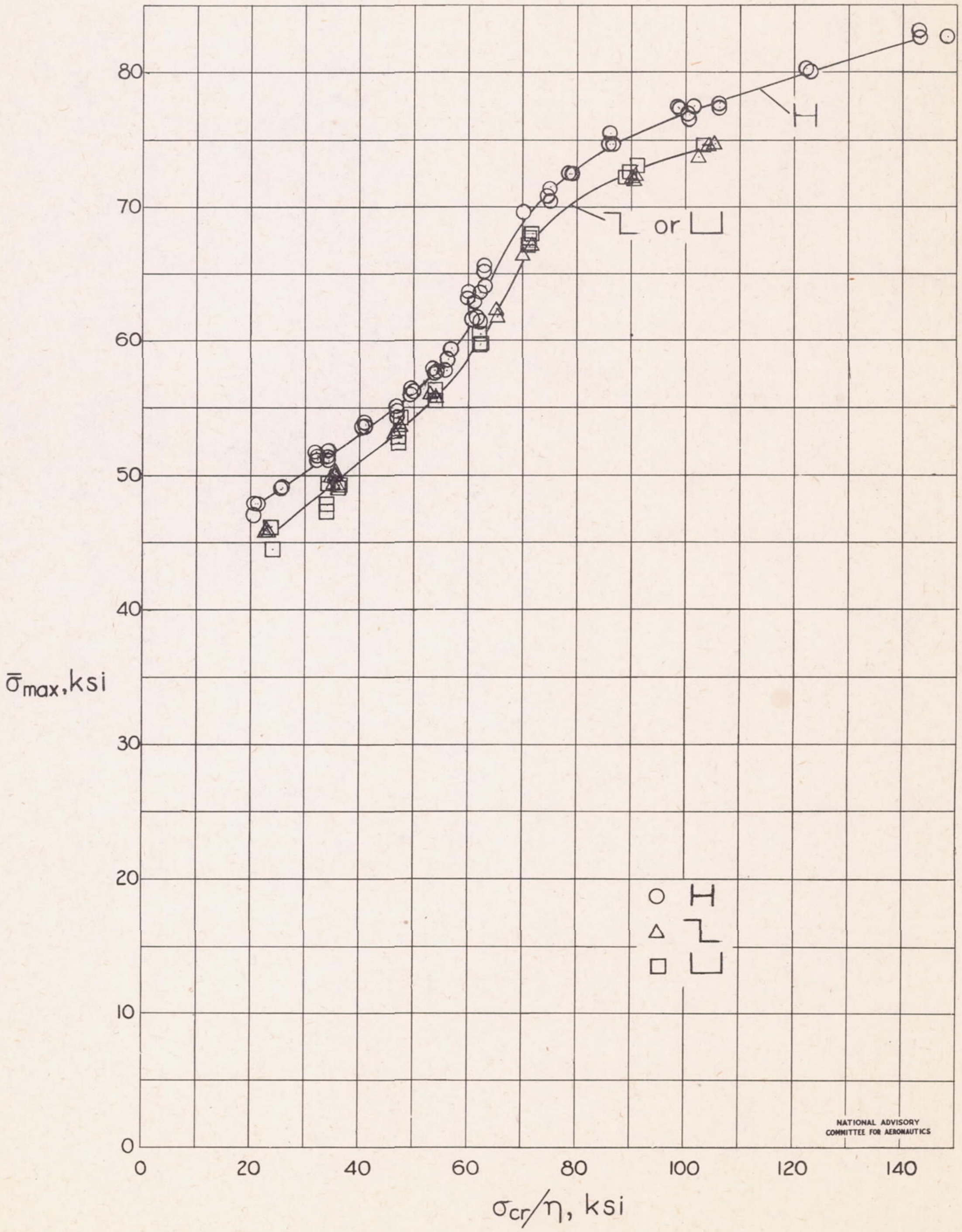

Figure 12.- Variation of $\bar{\sigma}_{max}$ with σ_{cr}/η for plates of extruded 75S-T aluminum alloy obtained from tests of H-, Z-, and channel-section columns. σ_{cy} = 79 ksi.